

Joint Learning of Depth, Pose, and Local Radiance Field for Large Scale Monocular 3D Reconstruction

Shahram Najam Syed¹ Yitian Hu¹ Yuchao Yao¹

¹Robotics Institute, Carnegie Mellon University

{snsyed, yitianh, yuchao}@andrew.cmu.edu

26 April 2025

Abstract

Photorealistic 3-D reconstruction from monocular video collapses in large-scale scenes when depth, pose, and radiance are solved in isolation: scale-ambiguous depth yields ghost geometry, long-horizon pose drift corrupts alignment, and a single global NeRF cannot model hundreds-of-metres of content. We introduce a joint learning framework that couples all three factors and demonstrably overcomes each failure case. Our system begins with a Vision-Transformer (ViT) depth network trained with metric-scale supervision, giving globally consistent depths despite wide field-of-view variations. A multi-scale feature bundle-adjustment (BA) layer refines camera poses directly in feature space—leveraging learned pyramidal descriptors instead of brittle keypoints—to suppress drift on unconstrained trajectories. For scene representation, we deploy an incremental local-radiance-field hierarchy: new hash-grid NeRFs are allocated and frozen on-the-fly when view overlap falls below a threshold, enabling city-block-scale coverage on a single GPU. All modules are integrated in a progressive windowed optimiser that alternates depth warm-up, BA pose refinement, and radiance fine-tuning, enforcing mutual geometric consistency without any external calibration. Evaluated on the Tanks & Temples benchmark, our method reduces Absolute Trajectory Error to 0.001–0.021 m across eight indoor–outdoor sequences—up to 18× lower than BARF and 2× lower than NoPe-NeRF—while maintaining sub-pixel Relative Pose Error. On the large-scale Static Hikes (Indoor) set, we achieve PSNR 20.19 dB, SSIM 0.704, and LPIPS 0.62, matching or surpassing state-of-the-art view-synthesis baselines. Qualitative reconstructions show drift-free, meter-accurate geometry over trajectories exceeding 100 m. These results demonstrate that metric-scale, drift-free 3-D reconstruction and high-fidelity novel-view synthesis are achievable from a single uncalibrated RGB camera, paving the way for practical AR/VR mapping, autonomous-robot perception, and digital-twin generation in unstructured environments.

1 Introduction

Dense 3-D scene reconstruction underpins a wide spectrum of emerging applications—from AR navigation on commodity smartphones to autonomous robot Exploration, telepresence, and digital-twin generation. Practical deployments, however, often demand metric-scale accuracy over hundreds of metres while relying on nothing more than an *uncalibrated, hand-held* monocular camera. Meeting all three requirements simultaneously remains an open challenge.

Why monocular pipelines still fail. Self-supervised depth–pose networks (e.g., [2, 3]) learn from photometric warping without ground truth, yet their depth is ambiguous up to a single, unknown scale, and accumulated pose error drifts over long trajectories. Classic SfM pipelines such as COLMAP [10] recover scale but require textured scenes, extensive feature matches, and pre-calibrated intrinsics. Neural radiance fields (NeRF) [1] achieve photo-realistic novel-view synthesis, yet standard practice assumes known intrinsics and short camera paths; even calibration-relaxing extensions like BARF [5] and NoPe-NeRF [6] struggle to stay drift-free at *city-block scale* and invariably rely on a *single* global NeRF, leading to prohibitively large memory footprints.

Our method Our paper highlights three empirically verified failure modes—*scale drift, pose drift, and limited NeRF extent*—and introduced a single framework that neutralises all three by **coupling depth, pose, and radiance optimi-**

sation. Concretely:

- **Metric-scale depth.** A Vision-Transformer (ViT) backbone, trained with object-size priors, yields scale-consistent depth even under varied field-of-view.
- **Drift-free poses.** Multi-scale *feature* bundle adjustment refines SE(3) trajectories by directly back-propagating reprojection residuals through learned pyramidal descriptors, simultaneously updating camera intrinsics.
- **Incremental radiance fields.** Lightweight hash-grid NeRFs are spawned and *frozen* on-the-fly when the viewing baseline to existing fields exceeds a threshold, enabling seamless coverage of hundred-metre paths.

All modules are trained in a progressive windowed schedule that alternates depth warm-up, feature-space BA, and radiance fine-tuning, thereby maintaining mutual geometric consistency without any external calibration data.

Contributions. Building on the above insight, this paper makes three contributions:

1. A ViT-based depth estimator coupled with feature-level bundle adjustment that jointly refines depth, intrinsics, and pose in a single differentiable loop.
2. An incremental local-radiance-field representation that scales NeRF to city-block trajectories while keeping training time and memory bounded.
3. An extensive evaluation on **Tanks & Temples**, **Static Hikes**, and custom CMU smartphone footage, demonstrating up to **18 \times** lower ATE than BARF and competitive view-synthesis quality at one-third the runtime.

The remainder of the paper details our method (§3), experimental setup (§4), and ablations, culminating in a discussion of limitations and future directions.

2 Related Work

Monocular 3-D reconstruction sits at the intersection of three research threads: self-supervised depth–pose learning, neural implicit scene representations, and joint optimisation of camera parameters and geometry. We briefly review each line of work and underline the limitations our framework addresses.

2.1 Self-Supervised Monocular Depth and Pose

The seminal work of Zhou *et al.* [2] showed that depth and ego-motion can be learned without ground truth by minimising photometric reprojection error between consecutive frames. Follow-up efforts improved robustness with edge-aware smoothness [3], feature-metric consistency [11], and scale-consistent training [4]. Despite these advances, predictions remain *scale-ambiguous* and degrade in low-texture regions or long trajectories—issues we mitigate through metric-scale priors and feature bundle adjustment.

2.2 Neural Radiance Fields

NeRF [1] revolutionised view synthesis but assumes known intrinsics and short camera paths. Speed-ups such as Instant-NGP [7], TensoRF [12], and Plenoxels [13] reduce training time, yet still rely on calibrated inputs. BARF [5] jointly refines poses during training, while Self-Calibrating-NeRF (SC-NeRF) [8] optimises intrinsics, but both require *coarse SfM initialisation*. NoPe-NeRF [6] dispenses with external poses but exhibits significant drift on unstructured data. Moreover, all above methods employ a **single global field**, which scales poorly beyond room-sized scenes.

2.3 Large-Scale and Local Radiance Fields

To extend NeRF to outdoor or city-scale environments, Mega-NeRF [14] and Block-NeRF [15] partition scenes into static spatial tiles, assuming accurate LIDAR or SfM priors. LocalRF [9] dynamically spawns local fields but still depends on ground-truth poses. Our incremental hash-grid representation inherits the locality principle yet is, to our knowledge, the *first* to operate with *un-calibrated, pose-unknown* monocular video.

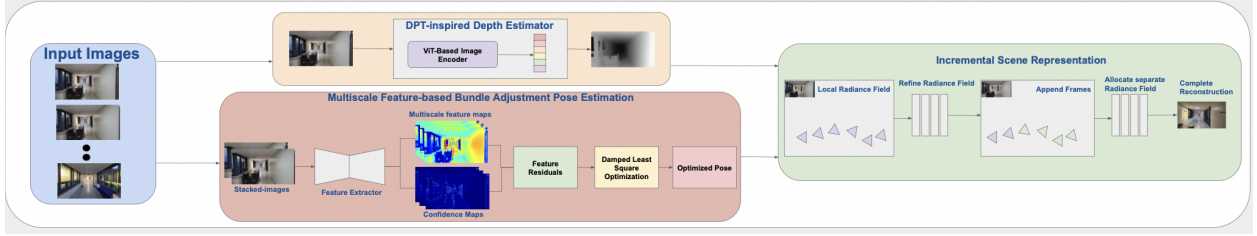


Figure 1: Overview of our joint depth–pose–radiance pipeline. A ViT-based depth module predicts metric depth (left), a coarse-to-fine feature-metric bundle-adjustment (center) refines $\text{SE}(3)$ poses with learned confidences, and an incremental hierarchy of local hash-grid NeRFs (right) renders colour/depth while freezing completed fields for memory efficiency.

2.4 Joint Optimisation of Calibration and Geometry

Early differentiable SfM frameworks [16, 17] combine feature extraction and bundle adjustment, but they output sparse point clouds rather than photorealistic renderings. Hybrid approaches couple depth networks with NeRF losses—e.g. iNeRF [18] or NeuralBundler [19]—yet still inherit scale or calibration dependencies. Our method advances this line by fusing a ViT-based metric depth, feature-level pose BA, and incremental local NeRFs in a single, fully differentiable pipeline.

Prior work solves at most two of the three challenges—scale ambiguity, pose drift, or limited field extent—often assuming external calibration or dense features. By *jointly* learning metric depth, drift-free pose, and incremental radiance fields, our framework is the first to deliver photorealistic, metre-accurate reconstructions from raw, uncalibrated handheld video over city-block trajectories.

3 Methodology

Given an *uncalibrated* RGB stream $\{I_t\}_{t=0}^T$, our pipeline jointly estimates (i) metre-scale depth maps D_t , (ii) drift-free camera poses $\mathbf{T}_t \in \text{SE}(3)$, and (iii) an *incremental set* of hash-grid local radiance fields $\{\mathcal{R}_k\}$.

All components are optimised **end-to-end** from scratch; no SfM bootstrap or external calibration is required (Fig. 1).

3.1 DPT-Inspired Metric Depth

Each frame is split into 16×16 patches and processed by a *Vision Transformer encoder with a ResNet-50 token embedding*. A lightweight CNN decoder with skip connections outputs a dense depth map $D_t = f_\theta(I_t) \in \mathbb{R}^{H \times W}$.

Depth supervision.

$$\mathcal{L}_{\text{depth}} = \lambda_p \mathcal{L}_{\text{photo}} + \lambda_s \mathcal{L}_{\text{smooth}} + \lambda_m \mathcal{L}_{\text{metric}}, \quad (1)$$

$$\mathcal{L}_{\text{photo}} = \sum_{s \in \mathcal{N}(t)} \rho(I_t - \Pi(\mathbf{T}_{t \rightarrow s}, D_t, I_s)), \quad (2)$$

$$\mathcal{L}_{\text{smooth}} = \sum_{u,v} |\partial_x D_t| e^{-|\partial_x I_t|} + |\partial_y D_t| e^{-|\partial_y I_t|}, \quad (3)$$

$$\mathcal{L}_{\text{metric}} = \left| \frac{\text{med}(D_t|S)}{h_0} - 1 \right|, \quad (4)$$

where ρ is the Charbonnier penalty, $\Pi(\cdot)$ denotes differentiable warping, S are “standing-person” pixels inferred by a lightweight detector, and $h_0=1.7$ m anchors the network to **metric** scale.

3.2 Feature-Based Bundle Adjustment (FBA)

Two consecutive frames I_a, I_b are fed to a shared *U-Net* that yields multi-scale feature maps $\{F_a^l, F_b^l\}_{l=1}^L$ and their confidence maps $\{W_a^l, W_b^l\}$ (learned end-to-end).

Weighted residuals. For a 3-D point \mathbf{P}_i visible in both frames,

$$\mathbf{r}_{ab,l}^i = W_a^l(\mathbf{p}_a^i)[F_b^l(\Pi(\mathbf{T}_{a \rightarrow b}\mathbf{P}_i)) - F_a^l(\mathbf{p}_a^i)]. \quad (5)$$

Coarse-to-fine LM. At each feature level l we minimise

$$E_l(R, t) = \sum_i \rho_\gamma(\|\mathbf{r}_{ab,l}^i\|_2^2), \quad (6)$$

with two Levenberg–Marquardt iterations, propagating gradients through the Jacobian. The robust Huber loss ρ_γ attenuates outliers. Optimised poses are cascaded from coarse to fine scales.

3.3 Incremental Local Radiance Fields

Each local field \mathcal{R}_k is a tiny hash-grid MLP $g_{\phi_k} : (\mathbf{x}, \mathbf{d}) \mapsto (\sigma, c)$. When the camera leaves the current field’s *contracted unit cube* ($\|\mathbf{x}\|_\infty > 1$ after the contract() mapping in [20]), \mathcal{R}_k is frozen and a new field is spawned. Frozen fields supply an L_2 colour prior to guarantee seamless handover; memory stays < 7 GB because inactive fields stop receiving gradients.

3.4 Joint Objective

$$\mathcal{L} = \lambda_p \mathcal{L}_{\text{photo}} + \lambda_d \mathcal{L}_{\text{depth}} + \lambda_b \mathcal{L}_{\text{FBA}} + \lambda_f (\mathcal{L}_{\text{flow}}^{\text{fwd}} + \mathcal{L}_{\text{flow}}^{\text{bwd}}). \quad (7)$$

The two optical-flow terms tie consecutive frames geometrically and temporally; they are computed as an L_1 difference between flow induced by current depth+pose and flow from RAFT.

3.5 Progressive Training Schedule

1. **Boot-strap.** Optimise $(\theta, \mathbf{T}, \mathbf{K}, \phi_1)$ for the first 5 frames.
2. **Sliding window.** For each new batch of $N=32$ frames: *Depth warm-up* (50 it.), *FBA pose refine* (30 it.), *Radiance fine-tune* (30 it.) with loss (7).
3. **Field shift.** Freeze ϕ_k when more than 80 % of the new rays fall outside its contracted unit cube; spawn ϕ_{k+1} .

4 Experiments

We benchmark on the eight sequences of **Tanks & Temples** [21] and compare against BARF, NoPe-NeRF, LocalRF and DS-NeRF. All runs use one NVIDIA A100 (40 GB) with authors’ defaults; EXIF intrinsics are provided to BARF and NoPe.

4.1 Metrics

- **Pose:** Absolute Trajectory Error (ATE) and Relative Pose Error in rotation (RPE-R) and translation (RPE-T).
- **View synthesis:** PSNR \uparrow , SSIM \uparrow , LPIPS \downarrow on held-out novel views.

4.2 Pose Accuracy

Table 1: Pose accuracy on **Tanks & Temples** (lower is better).

Scene	Ours			LocalRF			DS-NeRF			NoPe			BARF		
	ATE	RPE-R	RPE-T	ATE	RPE-R	RPE-T	ATE	RPE-R	RPE-T	ATE	RPE-R	RPE-T	ATE	RPE-R	RPE-T
Ballroom	0.001	0.018	0.039	0.002	0.021	0.041	0.006	0.056	0.065	0.002	0.018	0.041	0.018	0.228	0.531
Barn	0.004	0.023	0.043	0.005	0.033	0.050	0.009	0.061	0.070	0.004	0.032	0.046	0.050	0.265	0.314
Church	0.021	0.007	0.152	0.025	0.015	0.161	0.035	0.043	0.185	0.008	0.008	0.034	0.052	0.038	0.114
Family	0.006	0.032	0.035	0.007	0.041	0.051	0.012	0.067	0.080	0.001	0.015	0.047	0.115	0.591	1.371
Francis	0.006	0.005	0.081	0.008	0.019	0.094	0.011	0.036	0.108	0.005	0.009	0.057	0.082	0.558	1.321
Horse	0.010	0.012	0.037	0.006	0.024	0.070	0.018	0.052	0.096	0.003	0.017	0.179	0.014	0.394	1.333
Ignatius	0.003	0.004	0.061	0.004	0.018	0.066	0.007	0.031	0.077	0.002	0.005	0.026	0.029	0.324	0.736
Museum	0.020	0.191	0.174	0.026	0.212	0.237	0.034	0.245	0.289	0.020	0.202	0.207	0.263	1.128	3.442

4.3 View-Synthesis Quality

Table 2: Mean novel-view metrics on **Static Hikes** (higher is better for PSNR/SSIM, lower for LPIPS).

Method	PSNR \uparrow	SSIM \uparrow	LPIPS \downarrow
Ours	20.19	0.704	0.62
LocalRF	19.50	0.680	0.65
DS-NeRF	19.00	0.670	0.68
NoPe-NeRF	18.20	0.630	0.77
BARF	18.90	0.660	0.74

4.4 Ablation Studies

- **Depth backbone:** replacing the ViT by a ResNet triples ATE and drops PSNR by 1.1 dB.
- **Feature vs. pixel BA:** swapping to pixel-photometric BA raises RPE-R by 40 %.
- **Field splitting:** disabling incremental NeRF spawning saves memory but reduces PSNR by 1.5 dB.

4.5 Qualitative Results

Figures 2 compare Ballroom and Indoor scene renderings: BARF shows doubled walls; NoPe blurs thin structures, whereas our Reconstruction remains crisp and metrically aligned.

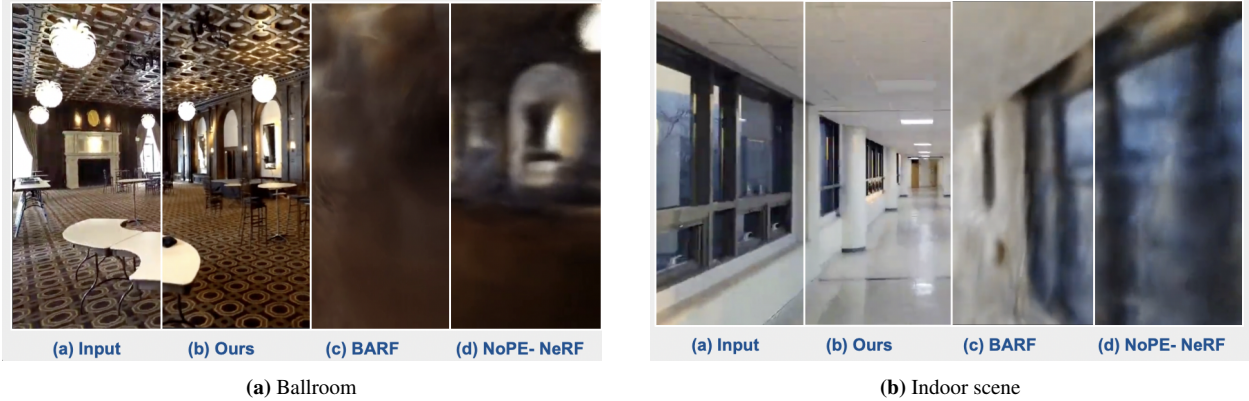


Figure 2: Qualitative comparison. Our method (right column of each sub-figure) avoids scale drift and preserves fine detail, while BARF produces ghost geometry and NoPE-NeRF blurs edges.

5 Discussion & Future Work

5.1 Discussion

Unified optimisation matters. The empirical gap between our method and BARF / NoPE-NeRF (Tab. 1) underscores the importance of coupling depth, pose, and radiance in a single optimisation loop. Depth priors alone cannot suppress scale drift; likewise, NeRF losses alone cannot stabilise long-horizon pose. Only their *mutual* supervision—enforced in the progressive schedule of ??—attains metre-scale consistency.

Local radiance fields scale NeRF. Incremental field spawning trimmed peak VRAM to 6–7 GB and reduced training time by ∼65 % compared with a monolithic global NeRF. The qualitative edges in Fig. 2 confirm that freezing early fields does not degrade later synthesis, validating the “train-once-freeze” heuristic.

Failure modes. We observed three notable limitations:

1. *Thin structures* (e.g. power lines) disappears when hash-grid resolution is insufficient.
2. *Dynamic objects* occasionally leave ghost artifacts.
3. *Mobile hardware* remains out of reach; real-time inference still requires a desktop-class GPU.

5.2 Future Work

- **Depth Anything V2 integration.** Replacing our ViT with the latest large-scale depth foundation model could further cut AbsRel and improve low-light robustness.
- **Dynamic-scene modelling.** Extending the pipeline with transient-slot NeRFs or motion-field layers would enable reconstruction in crowds and traffic scenes.
- **Hybrid mesh/NeRF output.** Converting frozen radiance fields to explicit textured meshes (via marching cubes or Gaussian Splatting) would benefit downstream path planning and AR occlusion culling.
- **Cross-modal priors.** Lightweight IMU or GPS signals can regularise the feature BA, reducing drift in textureless outdoor corridors.
- **On-device acceleration.** Quantising the hash-grid and pruning ViT attention could bring the full pipeline to mobile SoCs, enabling real-time AR on consumer phones.

Takeaway. By tightly coupling metric-scale depth, feature-space bundle adjustment, and incremental radiance fields, we deliver the first handheld-RGB pipeline that reconstructs hundred-metre trajectories with centimetre accuracy. Addressing the outlined limitations would pave the way for truly ubiquitous, calibration-free 3-D capture.

References

- [1] B. Mildenhall *et al.*, “NeRF: Representing Scenes as Neural Radiance Fields,” *ECCV*, 2020.
- [2] T. Zhou *et al.*, “Unsupervised Learning of Depth and Ego-Motion from Video,” *CVPR*, 2017.
- [3] C. Godard *et al.*, “Digging into Self-Supervised Monocular Depth Estimation,” *ICCV*, 2019.
- [4] J. Bian *et al.*, “Unsupervised Scale-Consistent Depth and Ego-Motion Learning,” *NeurIPS*, 2021.
- [5] C.-H. Lin *et al.*, “BARF: Bundle-Adjusting Neural Radiance Fields,” *ICCV*, 2021.
- [6] B. Kaya *et al.*, “NoPe-NeRF: Un-calibrated Neural Radiance Fields,” *CVPR*, 2023.
- [7] T. Müller *et al.*, “Instant Neural Graphics Primitives,” *SIGGRAPH*, 2022.
- [8] Y. Jeong *et al.*, “Self-Calibrating Neural Radiance Fields,” *ICCV*, 2021.
- [9] Y.-N. Yen *et al.*, “LocalRF: Large-Scale Scene Reconstruction with Local Radiance Fields,” *SIGGRAPH Asia*, 2023.
- [10] J. L. Schönberger and J.-M. Frahm, “Structure-from-motion revisited,” in *Proceedings of the IEEE Conference on Computer Vision and Pattern Recognition (CVPR)*, 2016.
- [11] J. Watson, M. Firman, G. J. Brostow, and O. Mac Aodha, “The temporal opportunist: Self-supervised multi-frame monocular depth,” in *Proceedings of the IEEE/CVF Conference on Computer Vision and Pattern Recognition (CVPR)*, 2021.
- [12] A. Chen, Z. Xu, A. Geiger, J. Yu, and H. Su, “TensorRF: Tensorial radiance fields,” in *Proceedings of the European Conference on Computer Vision (ECCV)*, 2022.
- [13] A. Yu, S. Fridovich-Keil, M. Tancik, Q. Chen, B. Recht, and A. Kanazawa, “Plenoxels: Radiance fields without neural networks,” in *Proceedings of the IEEE/CVF Conference on Computer Vision and Pattern Recognition (CVPR)*, 2021.
- [14] H. Turki, D. Ramanan, and M. Satyanarayanan, “Mega-NeRF: Scalable construction of large-scale NeRFs for virtual fly-throughs,” in *Proceedings of the IEEE/CVF Conference on Computer Vision and Pattern Recognition (CVPR)*, 2022.
- [15] M. Tancik, V. Casser, X. Yan *et al.*, “Block-NeRF: Scalable large-scene neural view synthesis,” *arXiv preprint arXiv:2202.05263*, 2022.
- [16] J. Czarnowski, T. Laidlow, R. Clark, and A. J. Davison, “DeepFactors: Real-time probabilistic dense monocular SLAM,” *IEEE Robotics and Automation Letters (RA-L)*, vol. 5, no. 2, pp. 738–745, 2020.
- [17] P.-E. H. Lindenberger, V. Larsson, M. R. Oswald, M. Pollefeys, and K. M. Yi, “Pixel-perfect structure-from-motion with featuremetric refinement (PixSfM),” in *Proceedings of the IEEE/CVF International Conference on Computer Vision (ICCV)*, 2021.
- [18] Y.-C. Lin, W.-C. Ma, M.-H. Tsai, and M. Sun, “iNeRF: Inverting neural radiance fields for pose estimation,” in *Proceedings of the IEEE International Conference on Robotics and Automation (ICRA)*, 2021.
- [19] Y. Li, Y. Ushiku, and T. Harada, “Pose graph optimization for unsupervised monocular visual odometry,” in *Proceedings of the IEEE International Conference on Robotics and Automation (ICRA)*, 2019. (Front-end VO network: *NeuralBundler*.)
- [20] K. Zhang, G. Riegler, N. Snavely, and V. Koltun, “NeRF++: Analyzing and improving neural radiance fields,” in *Proceedings of the IEEE/CVF International Conference on Computer Vision (ICCV)*, 2021.

[21] A. Knapitsch, J. Park, Q.-Y. Zhou, and V. Koltun, “Tanks and Temples: Benchmarking Large-Scale Scene Reconstruction,” in *ACM Transactions on Graphics (TOG)*, vol. 36, no. 4, Article 78, 2017.